JOURNAL OF THERMOPHYSICS AND HEAT TRANSFER
Vol. 11, No. 2, April–June 1997

Effects of Flowfield Nonequilibrium on Convective Heat Transfer to a Blunt Body

Tahir Gökçen*
NASA Ames Research Center, Moffett Field, California 94035

The axisymmetric Navier–Stokes equations are solved numerically for nonequilibrium airflows over a hemisphere. A formulation with a three-temperature thermochemical model has been employed to simulate vibrationally excited and partially dissociated airflow. A flow condition that has a total enthalpy of 25 MJ/kg and a surface pressure of 0.076 atm is studied. Computed stagnation point heat transfer using finite catalytic boundary conditions at the surface is compared with classical results. Departures from the classical heat transfer predictions caused by nonequilibrium effects are assessed for arcjet testing applications. A Damköhler number analysis is used to characterize the extent of flowfield nonequilibrium. It is shown that characterization of the thermodynamic state of the gas at the boundary-layer edge and within the boundary layer is needed to interpret the heat transfer measurements and to determine the surface catalytic efficiency.

Nomenclature

A_2 = generic diatomic molecule
c_i = mass fraction of species i
Da = Damköhler number
h_D = enthalpy contained in chemical mode
h_0 = total enthalpy
k_b = backward rate constant
k_f = forward rate constant
k_w = surface catalytic recombination rate
p = pressure
q = surface heat flux
R = nose radius of blunt body
$\mathcal{R}$ = reaction rate
s = distance along the surface
T = translational temperature
T_r = rotational temperature
T_v = vibrational–electronic temperature
u = x component of velocity
x_i = concentration of species i
γ = surface catalytic efficiency for recombination
μ = viscosity
ρ = density
ρ_i = density of species i
τ_{chem} = characteristic chemistry time
τ_{flow} = characteristic flow time
ς = Goulard parameter

Introduction

THIS investigation is a continuation of a previous study on nonequilibrium convective heat transfer to a blunt body.[1] The previous study concentrated on the validation of surface heat transfer rates and the exploration of a partial simulation concept. For relatively high Reynolds number flows, the nonequilibrium convective heat transfer computations were validated against the classical results of Fay and Riddell[2] and Goulard.[3] The previous work also showed that successful testing of convective heat transfer in an arcjet environment is possible with partial duplication of free-flight similitude variables. In the partial simulation, the duplication of surface pressure and total enthalpy of the free flight in an arcjet environment was sufficient to obtain similar convective heat transfer, provided that thermochemical equilibrium was reached at the edge of boundary layer. In other words, nonequilibrium convective heat transfer to a blunt body was not strongly dependent on freestream parameters.

To conduct the previous study, it was necessary to consider a hemisphere of 1 m radius so that the flow reached thermochemical equilibrium at the edge of the boundary layer. The present work investigates more realistic body sizes and Reynolds numbers that are encountered in an actual arcjet flow environment. Specifically, for practical sizes of test articles,[4,5] the density of the test flow and corresponding Reynolds numbers are such that thermochemical equilibrium may not be reached at the edge of the boundary layer and the boundary-layer flow may not be chemically frozen. One expects that this will cause departures from the convective heat transfer predicted by the Fay and Riddell[2] and Goulard[3] theory, since certain assumptions of the classical theory are not satisfied. The magnitude of these departures are of interest because the Fay and Riddell[2] and Goulard[3] formulas are used extensively in arcjet testing. The theory is frequently utilized to determine surface catalytic efficiency of heat-shield materials[6–10] and to estimate the total enthalpy of the test flow in arcjets,[11,12] and it is the basis of the partial simulation for heat transfer testing.[1]

The objective of this paper is to investigate the effects of thermochemical nonequilibrium, both at the edge of the boundary layer and within the boundary layer, on convective heat transfer to a blunt body with an emphasis on arcjet testing applications. In a case study, this paper attempts to isolate the effects of these nonequilibrium phenomena on the procedures for determining the surface catalytic recombination efficiency and total enthalpy of the test flow. The present approach is to compute flows over a hemisphere using the Navier–Stokes equations and compare the computed results with those predicted by the Fay and Riddell[2] and Goulard[3] formulas. Computed results using the partial simulation concept under nonequilibrium boundary-layer edge conditions will be presented. This paper will also give envelopes of frozen boundary-layer flow regime by means of Damköhler number analysis.

Presented as Paper 96-0352 at the AIAA 34th Aerospace Sciences Meeting and Exhibit, Reno, NV, Jan. 15–19, 1996; received Feb. 2, 1996; revision received Nov. 12, 1996; accepted for publication Dec. 12, 1996.

*Senior Research Scientist, Thermosciences Institute. Member AIAA.

Classical Theory and Its Applications

The classical result of Fay and Riddell[2] provides an analytical expression for convective heating to the stagnation point of a blunt body. For a fully catalytic surface with infinitely fast wall reactions, the heat transfer rate is given by

$$q_{k_w=\infty} = 0.763 Pr^{-0.6} (\rho_\delta \mu_\delta)^{0.4} (\rho_w \mu_w)^{0.1} \sqrt{\left(\frac{du_\delta}{dx}\right)_s} \times (h_{o\delta} - h_w) \left[1 + (Le^n - 1)\left(\frac{h_D}{h_{o\delta}}\right)\right] \quad (1)$$

where h_D is the energy contained in dissociation, the subscript w refers to the wall, the subscript δ refers to the edge of the boundary layer (Fig. 1), and the exponent n is 0.52 and 0.63 for equilibrium and frozen boundary layers, respectively. It is important to note here that since Le is of order unity for air, the heat flux given by Eq. (1) is not very sensitive to the boundary-layer thermochemistry as long as the recombination of atoms is completed at the wall.

Goulard,[3] allowing catalytic wall reactions to proceed at a finite speed, expressed the relative effect of finite wall reactions compared to infinitely fast wall reactions through a correction parameter

$$\bar{q} = q/q_{k_w=\infty} = 1 - \frac{Le^{2/3} h_D/h_{o\delta}}{1 + (Le^{2/3} - 1) h_D/h_{o\delta}} (1 - \varsigma) \quad (2)$$

where ς is given by

$$\varsigma = 1 \Big/ \left[1 + 0.47 Sc^{-2/3} \left(2\rho_\delta \mu_\delta \frac{du_\delta}{dx}\right)^{1/2} \Big/ (\rho_w k_w)\right] \quad (3)$$

Limitations and assumptions of the classical theory are summarized in Ref. 1 and are therefore not repeated here.

Applications of the Fay and Riddell[2] and Goulard[3] theory in arcjet testing include determination of the catalytic surface efficiency and total enthalpy of the test flow, and a partial simulation for convective heat transfer testing. The surface catalytic efficiency of heat-shield materials is determined by comparing the heat transfer rates of the sample material to that of a fully or noncatalytic material along with an analysis based on the Fay and Riddell[2] and Goulard[3] theory.[6–10] In these analyses, the catalytic recombination efficiency is obtained from the Fay and Riddell[2] and Goulard[3] formulas with the experimental measurements of surface heating rate, temperature, and pressure. Similarly, the total enthalpy of the flow in the test section is deduced using measurements of surface heating rate and pitot pressure, and a correlation based on the Fay and Riddell[2] and Goulard[3] theory.[11,12] The partial simulation concept explored in Ref. 1 for testing of surface heat transfer in a high-enthalpy tunnel is also based on the classical theory. A successful testing of free-flight convective heat transfer in an arcjet environment is possible with partial duplication of the free-flight similitude variables (e.g., duplication of the surface pressure and total enthalpy is sufficient when the flow is in equilibrium at the boundary-layer edge).

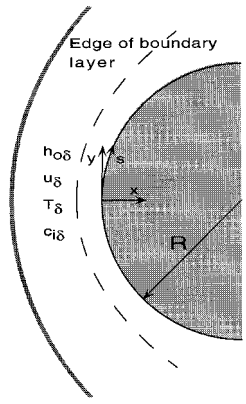

Fig. 1 Hypersonic flow over a hemisphere.

It is reasonable to assert that uncertainty exists concerning the accuracy of results obtained with these formulas in the environment of the arcjet wind tunnels where the assumptions leading to the theory are not satisfied. If these assumptions do not hold, there will be departures from the surface heat transfer computed using Eqs. (1–3), and in turn, there will be inaccuracy in the parameters predicted by the previous applications of the theory. The present work concentrates on the importance of the following two assumptions: 1) thermochemical equilibrium at edge of boundary layer and 2) chemically frozen boundary layer. A thermodynamic characterization of the flow is necessary to assess the extent of departures.

Thermodynamic Characterization of Flow

Thermodynamic characterization of a flowfield requires consideration of thermochemical processes occurring in the flowfield as well as the time scales of these processes relative to the flow time. The conditions under which a flowfield is in an equilibrium, frozen, or nonequilibrium state is determined by the Damköhler number associated with the gas-phase reactions.[2,3,13] By definition, when the time scale of gas-phase chemical reactions is large compared to the time scale of the flow, the flow is said to be chemically frozen. The opposite can be said for an equilibrium flow, and a nonequilibrium flow prevails when the time scales of flow and chemistry are of the same order.

In general, to characterize the flow with respect to one particular thermochemical process, a Damköhler number can be defined as

$$Da = \tau_{\text{flow}}/\tau_{\text{chem}} \quad (4)$$

Strictly speaking, Damköhler numbers for all processes must be considered for thermodynamic characterization of the flow. However, for dissociated airflows over a blunt body, the primary process is the dissociation–recombination reaction, i.e., for A_2 (N_2, O_2)

$$A_2 + M \rightleftharpoons 2A + M$$

where M represents a generic collision particle. If the chemical rate $\mathcal{R}$ is expressed in terms of forward and backward rate constants and species concentrations

$$\mathcal{R} = \sum_m (-k_{f_m} x_{A_2} x_m + k_{b_m} x_A^2 x_m) \quad (5)$$

then one can define the chemistry time as

$$1/\tau_{\text{chem}} = \mathcal{R}/x_T \quad (6)$$

where $x_T = \Sigma\, x_i$, and x_i is the concentration for species i. This definition of chemistry time has a singular point when concentration of species is the same as equilibrium composition or in equilibrium flow. However, for any near-equilibrium flow situations, forward and backward rates are so large that the chemistry time defined by Eq. (6) would still be much smaller than flow time.

For the boundary layer, the flow time is appropriately defined using the velocity gradient at the edge of boundary layer

$$\tau_{\text{flow}} = \left(\frac{\partial u}{\partial x}\right)_{e,s}^{-1} \simeq R \left(\frac{\rho}{2p}\right)_\delta^{1/2} \quad (7)$$

where the velocity gradient is approximated by the stagnation point flow and Newtonian theory.[2]

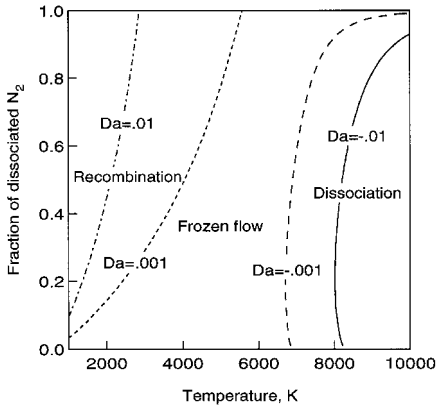

Fig. 2 Flow regimes of N_2 dissociation–recombination for a blunt body of 5.08-cm nose radius at p_s = 0.076 atm.

The Damköhler number, using Eqs. (6) and (7), can then be expressed as

$$Da = (\mathcal{R}/x_T)R(\rho/2p)_s^{1/2} \tag{8}$$

where negative values of Da correspond to dissociation-dominated flows and positive values of Da correspond to recombination-dominated flows.

The frozen-flow regime exists when the Damköhler number is much smaller than unity ($|Da| \leq 0.01$). In general, $\mathcal{R}$ is a function of internal temperatures (T and T_v) and species concentrations. If the temperatures are assumed to be equilibrated, using Eq. (8) one can generate an envelope of frozen flow regime where $|Da| \leq 0.01$. For flows over a hemisphere of 5.08 cm radius and p_s = 0.076 atm, such an envelope of frozen flow for N_2 dissociation–recombination reaction is shown in Fig. 2.

Figure 2 indicates that the temperature range for frozen boundary layer decreases significantly as the dissociation level increases. Therefore, to determine whether a boundary-layer flow is frozen to recombination, the dissociation level in the boundary-layer flow must be known. For a particular size of test article, when the boundary-layer edge conditions are known, this kind of plot can be utilized to determine whether the boundary-layer flow is frozen or not.

Formulation

An axisymmetric nonequilibrium formulation is employed for computations of viscous blunt body flows of air. The nonequilibrium air model used in Ref. 1 is modified to include argon for arcjet flow environments. The current model has 12 chemical species (N_2, O_2, NO, N, O, N_2^+, O_2^+, NO^+, N^+, O^+, e^-, and Ar), and the thermal state of the gas is described by three temperatures: 1) translational, 2) rotational, and 3) vibrational–electronic. The governing Navier–Stokes equations are supplemented with the equations accounting for thermochemical nonequilibrium processes and solved numerically using an implicit finite volume method. Although rotational nonequilibrium is allowed in the formulation, for computations presented in this paper, translational and rotational energy modes are assumed to be in equilibrium, and the two-temperature model of Park[14] is employed for the reactions and rate coefficients. More information on the thermochemical model and computational code can be found in Ref. 1.

Presentation of Results

The axisymmetric flows with nonequilibrium thermochemistry over different radii sphere–cylinders are computed at two flow conditions corresponding to a total enthalpy of 25 MJ/kg and surface pressure of 0.076 atm. These conditions are taken from Ref. 1. One flow condition corresponds to a typical arcjet test flow where the freestream is in a nonequilibrium state, and the other corresponds to free flight where the freestream is air at standard atmospheric conditions. The equivalent freestream conditions for arcjet flow and free flight are determined in such a way that the total enthalpy of the flow and surface pressure are duplicated approximately. The flight condition corresponds to that of approximately 65-km Earth altitude. The surface pressure and freestream conditions are summarized in Table 1.

All computations presented in this paper used a 60 × 80 grid (80 points normal to the wall). From a grid refinement study in Ref. 1, this grid resolution is concluded to be sufficient for accurate heat transfer computations.

Computations are carried out for two nose radii of 1 m and 5.08 cm. At the surface, a fixed wall temperature of 1000 K and finite catalytic boundary conditions are prescribed. These conditions, along with the two nose radii, cover sufficiently broad time scales for thermochemistry and flow so that computational results can be used to investigate effects of nonfrozen boundary layer, nonequilibrium at edge of the boundary layer, and the partial simulation concept for heat transfer testing.

Nonfrozen Boundary Layer

The flow over a hemisphere of 1 m radius is used as a benchmark because the computed heat transfer for a fully catalytic surface has been validated against the classical results of Fay and Riddell[2] and Goulard[3] in Ref. 1. In Fig. 3, taken from Ref. 1, the computed surface heat transfer (labeled qtot) for the arcjet flow is compared against the heat transfer predicted by the Fay and Riddell[2] and Goulard[3] theory (labeled FRG). The transport properties and velocity gradient at the edge of the boundary layer in Eqs. (1–3) are determined from the computed flowfield. The edge of the boundary layer is defined with respect to the total enthalpy of the flow, and the species, velocity, and temperature boundary layers are not distinguished. In the computed flowfield the edge of the boundary

Table 1 Surface pressure and freestream conditions for the free flight and arcjet flow

Parameter	Free flight	Arcjet
h_o, MJ/kg	25.21	25.05
p_s, atm	0.0758	0.0762
Re_∞, (R = 1 m)	7145.9	3479.1
u_∞, m/s	7070	5630
p_∞, Pa	10.11	96.12
ρ_∞, kg/m^3	1.600×10^{-4}	2.546×10^{-4}
T_∞, K	220	970
$T_{v\infty}$, K	220	2800
$c_{N_2\infty}$	0.7381	0.6274
$c_{O_2\infty}$	0.2619	0
$c_{NO\infty}$	0	0
$c_{N\infty}$	0	0.1104
$c_{O\infty}$	0	0.2622

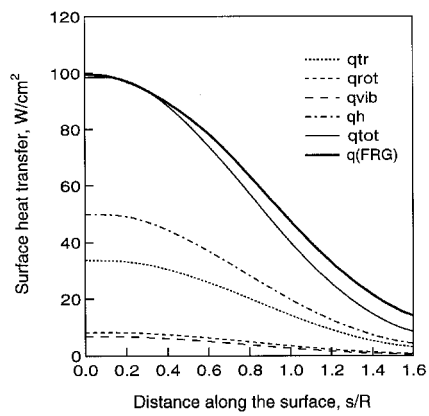

Fig. 3 Validation of computed heat transfer against the classical theory; a 1-m-radius hemisphere with a fully catalytic surface.

layer is determined as the location where the total enthalpy is within 1% of the freestream total enthalpy and does not vary more than 0.5% between the adjacent grid points. Although strict comparison with the theory is only valid at the stagnation region, the classical theory here is employed away from the stagnation point using the local velocity gradient and flow properties at the edge of the boundary layer. In Fig. 3, the separate contributions of the conduction and diffusion components of the computed heat flux are also presented. The diffusive heat flux q_h is of interest because this is the component of heat transfer that can be eliminated (or reduced) using a noncatalytic surface when the boundary layer is chemically frozen (or in nonequilibrium).

Figure 4 shows the computed stagnation streamline profiles for the noncatalytic surface for the arcjet condition of Fig. 3. The flow behind the shock reaches thermochemical equilibrium at the edge of the boundary layer, which can be inferred from the relatively flat region between the shock and the body in Fig. 4. Also, nonfrozen chemistry of nitrogen recombination within the boundary layer is clear from the atomic species profiles shown in Fig. 4b.

To investigate the thermodynamic state of the gas in the boundary layer, the frozen boundary-layer envelopes are computed. Envelopes for N_2 and O_2 dissociation–recombination for the 1-m nose radius body at a surface pressure of p_s = 0.076 atm are shown in Figs. 5 and 6, respectively. From Fig. 5, the envelope of frozen boundary-layer flow for N_2 recombination at temperatures less than 6000 K is largest when the fraction of dissociated N_2 molecules is small (i.e., $\leq$10%). The computed stagnation point boundary-layer profile of atomic nitrogen for the noncatalytic surface is also presented in Fig. 5. It is clear that much of the boundary-layer profile does not lie in the frozen flow regime. Note that the fraction of dissociated N_2 is equivalent to the mass fraction of N for N_2 and N mixtures, but not for air.

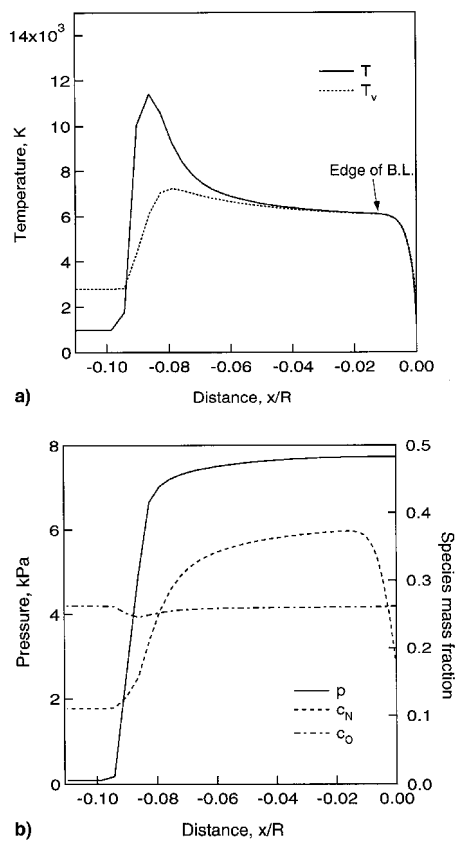

Fig. 4 Computed stagnation streamline profiles; arcjet flow over a hemisphere of 1 m radius: a) temperature profiles and b) pressure and atomic mass fraction profiles.

Although the nearly constant atomic oxygen profile in Fig. 4b appears to be frozen, examination of Fig. 6 indicates that the boundary-layer flow is not frozen to the recombination of O_2 within the temperature range of the boundary-layer flow. Instead, O_2 is fully dissociated and will stay that way at the boundary-layer temperatures of this case.

Since the assumption of thermochemical equilibrium at the edge of the boundary layer is satisfied for the arcjet flow over a 1-m nose radius body, flowfield computations for several surface catalytic efficiencies are made to show the effect of a nonfrozen boundary layer on the heat transfer.

Figure 7 shows the comparison of the computed and theoretical heat fluxes as a function of surface catalytic efficiency. The fluxes are normalized by the fully catalytic value (γ = 1).

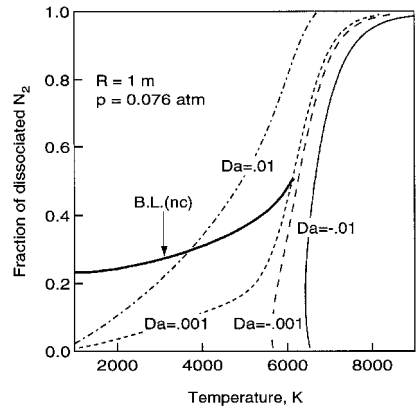

Fig. 5 Envelope of frozen boundary layer for N_2 dissociation–recombination at p_s = 0.076 atm.

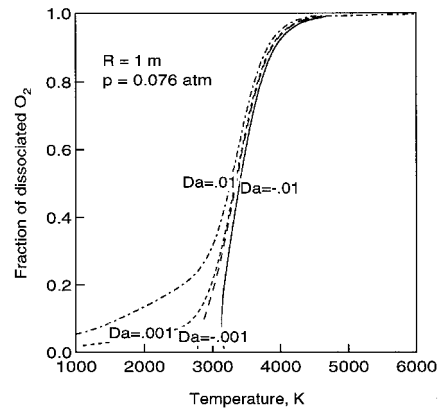

Fig. 6 Envelope of frozen boundary layer for O_2 dissociation–recombination at p_s = 0.076 atm.

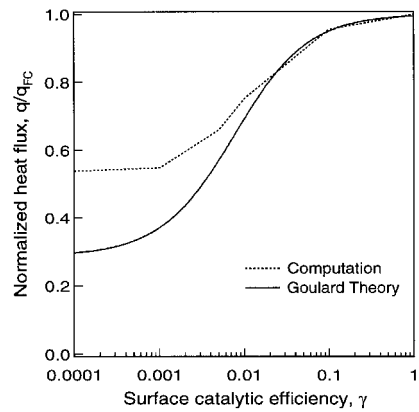

Fig. 7 Effect of nonfrozen boundary layer on surface heat transfer.

The theoretical curve is generated using Eqs. (2 and 3), where the flow properties and velocity gradient at the edge boundary layer are taken from the computed flowfield with a fully catalytic surface. In Fig. 7 it is deduced that most of the departure from the classical theory is because of nonequilibrium in the boundary layer since thermochemical equilibrium condition at the boundary-layer edge is satisfied.

There are two important consequences of nonequilibrium or nonfrozen boundary layer:

1) The full classically predicted reduction in the surface heat transfer through the use of a noncatalytic surface is not realized (if a spacecraft is flying in a flow regime where the boundary layer is not frozen, the use of noncatalytic tiles will only partially reduce the surface heat transfer).

2) If the surface catalytic efficiency is determined from the heat transfer measurements and the theoretical curve, the catalytic efficiency values will be significantly overestimated.

Nonequilibrium at Boundary-Layer Edge

Reducing the nose radius of the hemisphere while keeping the freestream conditions fixed has the following two effects on the flowfield thermochemistry:

1) The flow becomes out of thermochemical equilibrium at the edge of boundary layer.

2) The flow in the boundary layer becomes more chemically frozen.

For the 5.08-cm nose radius hemisphere, it is observed that the flow is approximately frozen in the boundary layer and out of equilibrium at the edge of boundary layer. This body size is typical for articles tested in arcjets, and is used here to investigate effects of nonequilibrium at edge of the boundary layer on heat transfer and to test the partial simulation concept under nonequilibrium boundary-edge conditions.

Two sets of computations are carried out for the 5.08-cm-radius hemisphere: one set corresponding to an arcjet wind-tunnel flow and the other corresponding to free flight. The computed stagnation streamline profiles for the two free-streams using a noncatalytic surface condition are presented in Figs. 8 and 9. For both cases, it is readily observed that the flow does not have an equilibrium region between the shock and the body, and there is significantly less dissociated nitrogen at the edge of the boundary layer in comparison with the flowfield over a 1-m hemisphere. Since the flow is not in equilibrium at the edge of the boundary layer, the distribution of total enthalpy among internal energy modes and chemical mode are different from that of the 1-m nose radius case. From the boundary-layer profiles of atomic nitrogen and oxygen in Figs. 8b and 9b, it can be inferred that the gas chemistry of recombination is approximately frozen since the atomic species concentrations remain relatively constant across the boundary layer for noncatalytic boundary conditions.

To verify the existence of a frozen boundary layer over a hemisphere of 5.08 cm radius at p_s = 0.076 atm, the frozen flow envelopes for N_2 and O_2 dissociation–recombination reactions are shown in Figs. 10 and 11, respectively. From Fig. 10 it is deduced that a boundary-layer flow will be frozen to N_2 dissociation–recombination (i.e., $|Da| \leq 0.01$) for temperatures between 2000–8000 K, regardless of how many N_2 molecules are dissociated. Added to Fig. 10 are the computed stagnation point boundary-layer profiles of atomic nitrogen for both the arcjet flow and free flight, which lie in the frozen boundary-flow regime for N_2 recombination. On the other hand, from Fig. 11, O_2 recombination will not be frozen in the boundary layer unless all O_2 molecules are dissociated (or the temperature is between 2000–4000 K). Again, O_2 is fully dissociated through most of the boundary layer as for the 1-m sphere case in Fig. 6.

For the 5.08-cm nose radii cases, the computed heat transfer cannot be directly compared against the classical theory since

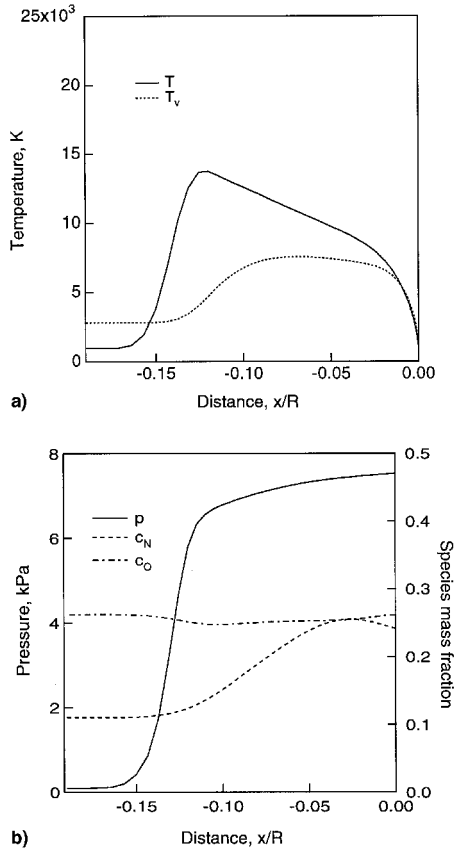

Fig. 8 Computed stagnation streamline profiles; arcjet flow over a hemisphere of 5.08 cm radius: a) temperature profiles and b) pressure and atomic fraction profiles.

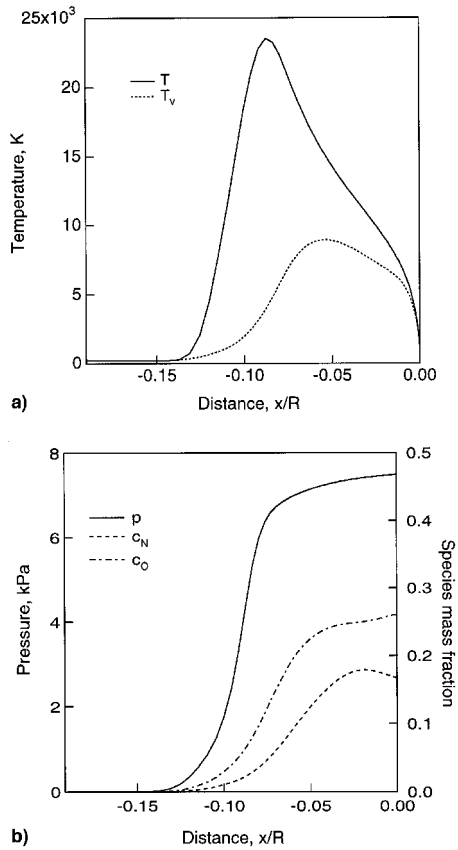

Fig. 9 Computed stagnation streamline profiles; free-flight flow over a hemisphere of 5.08 cm radius: a) temperature profiles and b) pressure and atomic fraction profiles.

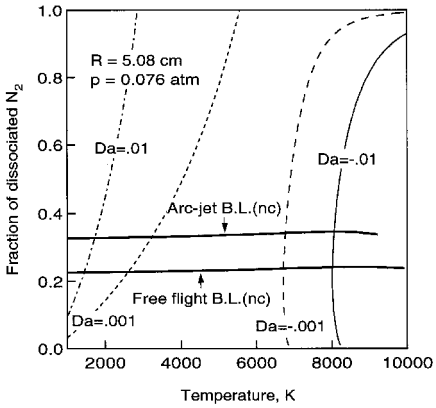

Fig. 10 Envelope of frozen boundary layer for N_2 dissociation–recombination at p_s = 0.076 atm.

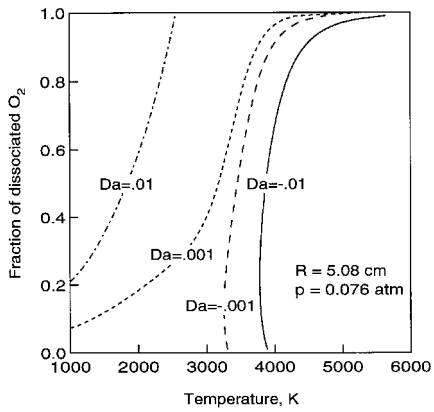

Fig. 11 Envelope of frozen boundary layer for O_2 dissociation–recombination at p_s = 0.076 atm.

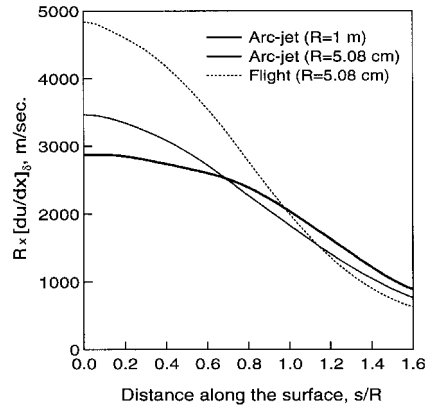

Fig. 12 Comparison of velocity gradients at the edge of boundary layer.

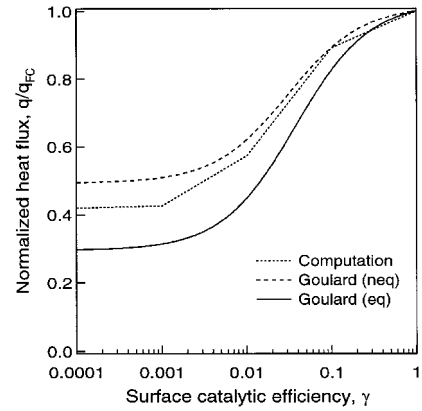

Fig. 13 Effect of nonequilibrium at the edge of boundary layer on heat transfer for the arcjet flow.

the flow is not in equilibrium at the edge of the boundary layer. However, one can make use of the 1-m and 5.08-cm nose radii solutions to test some classical results.

One can test whether the velocity gradient at the edge of the boundary layer varies inversely proportional to the nose radius, which is a well-known result from the stagnation point flow and Newtonian theory. Figure 12 shows the product of R and the computed velocity gradients at the edge of the boundary layer for the 5.08- and 1-m nose radii. For the two arcjet cases, velocity gradients scale reasonably well with $1/R$. However, for the free-flight case, the velocity gradient is much larger than that of the arcjet flow. This is mostly attributable to the smaller shock standoff distance for the free flight. A similar observation was made in Ref. 1 for the 1-m-radius body.

Flowfield computations for the 5.08-cm nose radius at several surface catalytic efficiencies are made to show the effect of nonequilibrium at the edge of boundary layer on the surface heat transfer. The normalized computed heat flux for the arcjet flow as a function of surface catalytic efficiency is compared with the Goulard theory in Fig. 13. The two theoretical curves are computed using Eqs. (2) and (3). The one labeled (neq) uses the flow properties and velocity gradient at the edge of boundary layer from the computed arcjet flowfield of the 5.08-cm sphere with the fully catalytic surface, and the other labeled (eq) uses the postshock equilibrium flow properties at the edge of boundary layer and the velocity gradient from the computed flowfield. A condition of nonequilibrium at the edge of boundary layer is not a unique condition, for this particular case, since the flow has less dissociation than the flow in equilibrium, the nonequilibrium at the edge of the boundary layer lessens the effect of surface catalysis on heat transfer. The computations are in reasonable agreement with the Goulard theory when the nonequilibrium edge boundary conditions are used in Eqs. (2) and (3), except for a departure at low catalytic efficiencies. This departure is probably caused by the small degree of nonequilibrium still present in the boundary layer. It should be noted that if the surface catalytic efficiency is determined from the heat transfer measurements and the theoretical curve (eq), large errors in the catalytic efficiency will be introduced because of nonequilibrium at the edge of the boundary layer.

Partial Simulation

For the 5.08-cm hemisphere, to explore the partial simulation concept, similar computations are carried out with the free-flight freestream conditions. The computed heat fluxes for fully catalytic and noncatalytic walls are presented in Fig. 14. For the fully catalytic wall case, the agreement between the arcjet flow and free flight is reasonably good, and partial duplication of enthalpy and pressure provides adequate simulation. The discrepancy at the stagnation point is mostly attributed to the different velocity gradients resulting from different shock standoff distances. For the noncatalytic wall case, the heat flux for free flight is significantly larger than that for the arcjet flow. To explain this difference for the noncatalytic case, the conduction and diffusion components of the heat flux for the fully catalytic case are presented in Fig. 15. Even though the total heat fluxes are similar for both the arcjet flow and free flight (Fig. 14), the diffusive heat flux for the arcjet flow is considerably larger since there is more dissociation at the edge of the boundary layer. Conversely, the internal energy component of the free-flight enthalpy at the boundary-layer edge is much larger than that of the arcjet flow. Since surface catalycity has an effect on only the chemical mode of the total enthalpy or on the diffusive flux, the noncatalytic heat flux becomes most sensitive to the degree of nonequilibrium at the boundary-layer edge in the partial simulation.

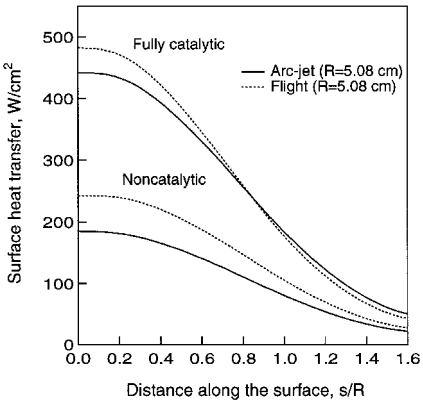

Fig. 14 Comparison of computed fully catalytic and noncatalytic heat fluxes for the arcjet flow and free flight.

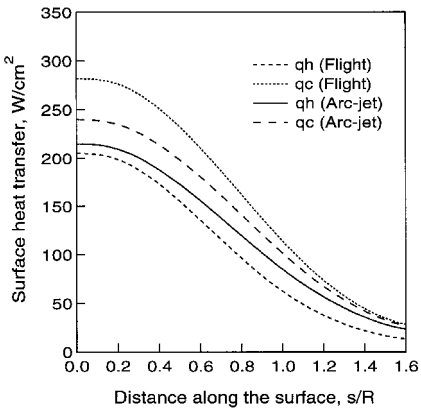

Fig. 15 Comparison of fully catalytic heat flux components for the arcjet flow and free flight.

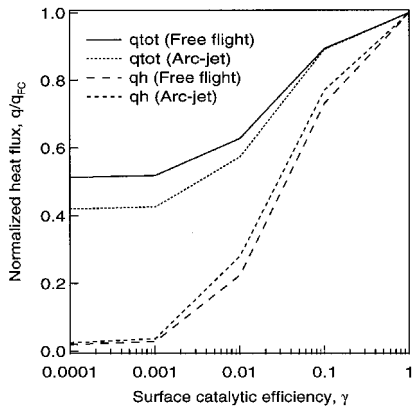

Fig. 16 Scaling of diffusive and total heat flux for flows over the 5.08-cm-radius hemisphere.

Finally, the normalized total and diffusive heat flux for the arcjet flow and free flight are compared in Fig. 16. Again, since surface catalycity has an effect on only the chemical mode, the normalized diffusive fluxes vary similarly with the catalytic efficiency, whereas the total heat fluxes do not. The implication is that one needs to reproduce the diffusive flux as well as the total heat flux to reproduce the surface catalytic effects accurately. In other words, for the partial simulation in a nonequilibrium environment of arcjets, in addition to duplication of the total enthalpy and surface pressure, the dissociation level at the edge of the boundary layer must be equal to that of flight. This condition is automatically satisfied when the flow is in thermochemical equilibrium at the boundary-layer edge.

Concluding Remarks

The present work is a case study attempting to isolate effects of the nonequilibrium phenomena such as nonfrozen boundary layer and nonequilibrium at the edge of the boundary layer on convective heat transfer to a blunt body, and to test the partial simulation concept for heat transfer testing. Departures from the classical heat transfer predicted by the Fay and Riddell[2] and Goulard[3] theory because of these nonequilibrium effects are assessed. It is shown here that characterization of the arcjet flow, thermodynamic state of the gas at the edge of the boundary layer and within the boundary layer is very important to interpret the heat transfer measurements and to determine the surface catalytic efficiency. One can not accurately interpret surface catalysis experiments in arcjets without understanding flowfield nonequilibrium. Computational and experimental efforts should be directed to characterize the freestream flow and shock layer in the existing arcjet test facilities. In the arcjet flow environment where the Fay and Riddell[2] and Goulard[3] theory is not applicable, a validated computational fluid dynamics code should play an important role in characterization of the flow and determination of the surface catalytic efficiency.

Acknowledgment

The author acknowledges the support of the Reacting Flow Environments Branch at NASA Ames Research Center through Contract NAS2-14031 to the Eloret Institute.

References

[1]Gökçen, T., "Effects of Freestream Nonequilibrium on Convective Heat Transfer to a Blunt Body," *Journal of Thermophysics and Heat Transfer*, Vol. 10, No. 2, 1996, pp. 234–241.

[2]Fay, J. A., and Riddell, F. R., "Theory of Stagnation Point Heat Transfer in Dissociated Air," *Journal of the Aerospace Sciences*, Vol. 25, No. 2, 1958, pp. 73–85.

[3]Goulard, R., "On Catalytic Recombination Rates in Hypersonic Stagnation Heat Transfer," *Jet Propulsion*, Vol. 28, No. 11, 1958, pp. 733–745.

[4]Pope, R. B., "Stagnation-Point Convective Heat Transfer in Frozen Boundary Layers," *AIAA Journal*, Vol. 6, No. 4, 1968, pp. 619–626.

[5]Anderson, L. A., "Effect of Surface Catalytic Activity on Stagnation Heat-Transfer Rates," *AIAA Journal*, Vol. 11, No. 5, 1973, pp. 649–656.

[6]Scott, C. D., "Catalytic Recombination of Nitrogen and Oxygen on High-Temperature Reusable Surface Insulation," AIAA Paper 80-1477, July 1980.

[7]Stewart, D. A., Kolodziej, P., and Leiser, D. B., "Effect of Variable Surface Catalysis on Heating near the Stagnation Point of a Blunt Body," AIAA Paper 85-0248, Jan. 1985.

[8]Kolodziej, P., and Stewart, D. A., "Nitrogen Recombination on High-Temperature Reusable Insulation and the Analysis of Its Effect on Surface Catalysis," AIAA Paper 87-1637, June 1987.

[9]Clark, R. K., Cunnington, G. R., Jr., and Wiedemann, K. E., "Determination of the Recombination Efficiency of Thermal Control Coatings for Hypersonic Vehicles," *Journal of Spacecrafts and Rockets*, Vol. 32, No. 1, 1995, pp. 89–96.

[10]Stewart, D. A., Chen, Y. K., Bamford, D. J., and Romanovsky, A. B., "Predicting Material Surface Catalytic Efficiency Using Arc-Jet Tests," AIAA Paper 95-2013, June 1995.

[11]Pope, R. B., "Measurements of Enthalpy in Low-Density Arc-Heated Flows," *AIAA Journal*, Vol. 6, No. 1, 1968, pp. 103–110.

[12]Scott, C. D., "Survey of Measurements of Flow Properties in Arcjets," *Journal of Thermophysics and Heat Transfer*, Vol. 7, No. 1, 1993, pp. 9–24.

[13]Grier, N. T., and Sands, N., "Regime of Frozen Boundary Layers in Stagnation Region of Blunt Reentry Bodies," NASA TN D-865, May 1961.

[14]Park, C., "Review of Chemical-Kinetic Problems of Future NASA Missions, I: Earth Entries," *Journal of Thermophysics and Heat Transfer*, Vol. 7, No. 3, 1993, pp. 385–398.